

## MOLECULAR STRUCTURE, NBO AND HOMO-LUMO ANALYSIS OF QUERCETIN ON SINGLE LAYER GRAPHENE BY DENSITY FUNCTIONAL THEORY

M. SARANYA<sup>a</sup>, S. AYYAPPAN<sup>a\*</sup>, R. NITHYA<sup>a</sup>, R. K. SANGEETHA<sup>b</sup>  
A. GOKILA<sup>b</sup>

<sup>a</sup>*Department of Physics, Government college of Technology, Coimbatore, 641013, India*

<sup>b</sup>*Department of Physics, Sri Eshwar College of Engineering, Coimbatore, 608002, India*

Quercetin (3,5,7,3',4'- pentahydroxyflavone) is a member of flavonoids. Density functional theory has been employed to study the adsorption of quercetin on single layer graphene (QCT-SLG) was investigated with the basis set of 6-21G. The total density of states and partial density states of the titled molecules were performed at density functional theory method. The molecular electrostatic potential (MEP) mapping shows the binding interactions of quercetin with single graphene layer. Dipole moment, hyperpolarizability and quantum chemical parameters have been calculated by Hartree Fock (HF) approximation approach. The natural bonding orbital analyses (NBO) calculation confined that the occurrence of intramolecular charge transfer takes place within the molecules. From DFT, highest occupied molecular orbital (HOMO) and lowest unoccupied molecular orbital (LUMO) energy levels of frontier orbital were obtained.

(Received October 13, 2017; Accepted January 15, 2018)

*Keywords:* QCT-SLG, Density Functional Theory, Hartree Fock, Molecular electrostatic potential, Natural Bonding orbital, HOMO-LUMO

### 1. Introduction

Flavonoids are the most important class of polyphenolic compounds, which in addition to their important biological roles in plant pigmentation, nitrogen fixation, and chemical defense possess anti-cancer, anti-inflammatory, antibacterial, antiviral, and antiallergic properties that are a consequence of their antioxidant properties [1]. Flavonoids, found in leaves, barks, rinds, seeds, and flowers- frequently closely associated with Vitamin C and offering synergistic effects. Both flavonoids and vitamin C benefit plants by providing them with antioxidant protection and are also important for human health. Quercetin is a strong hydroxyantioxidant and major dietary flavonoid (flavonols) most common present in nature [2-4]. Hydroxy and oxy groups present in a quercetin structure have the ability to form complexes with various oxygen groups. It was commonly found in plants and fruits. Quercetin is the most abundant of the flavonoids –which has 3 rings and 5 hydroxyl groups. Quercetin is found in many common foods including apple, tea, onion, nuts, berries, cauliflower, cabbage. Graphene, a single carbon layer with oxygen based functional groups bonded across the surface. The analysis of the interaction mechanism between flavonol molecules and the graphene surface has also led to relevant studies with regard to interaction energies and charge transfer between the molecules, structural changes and chemical properties of adsorbed molecules. Graphene is being focused for the scientific community due to its great potential in many applications such as biotechnology, nanobiomedicine or electronic devices [5-9]. The potential applications of graphene might open through chemical functionalization such as adsorption of molecules [10].

---

\*Corresponding author: ayyappan@gct.ac.in

As a matter of fact, the functionalization and modification of graphene properties, with particular attention to the zero-gap band behavior, through covalent and non-covalent interactions with adsorbed moieties have a greater attention. Non-covalent interactions between organic molecules and the graphene surface lead to very subtle effects on the graphene  $\pi$ -electronic structure, rising from vander Waals forces,  $\pi$ - $\pi$  interactions and several other effects [11,12]. The charge transfer between electron donating or accepting adsorbed molecules and graphene induces changes in the carriers in graphene called molecular doping is a relevant approach to modify electronic properties of graphene [13-21]. The investigation of the interaction mechanism between flavonol molecules and the graphene surface has also led to relevant studies with regard to interaction energies and charge transfer as a function of the molecular structure and properties of adsorbed molecules [8-11, 17-36]. The influence of the adsorbed molecule on electronic properties of graphene is strongly depends upon their respective properties and their mutual interactions. However, it is difficult to predict which molecules could lead to new systems with the desired features. The theoretical calculations (such as density functional theory, DFT) are very useful tool to identification and quantification of the interactions between adsorbed molecules and graphene. Recently, density functional theory (DFT) method, have performed to evaluated chemical properties, Subsequently, the study of the electronic and molecular properties is one of the greater importance that helps to investigate the mechanism of the antioxidant activity of these compounds. Density functional theory (DFT) was used to study the adsorption of flavonols on the graphene surface, focusing our interest on flavonol features. Electronic properties such as electron affinity (EA), hardness ( $\eta$ ), softness (S), electronegativity ( $\chi$ ) and electrophilic index ( $\omega$ ) are also evaluated. The frontier molecular orbitals (FMOs) and band gap energies are constructed and analyzed. The molecular electrostatic potential (MEP) showed that the reactive site for electrophilic and nucleophilic attacks and charge delocalization is characterized using natural bond orbital (NBO) analysis. Density of states (DOS), Projected Density of states (PDOS), Orbital Projected Density of states (OPDOS) for occupied and unoccupied molecular orbital is interpreted [37]. The present investigation gives a detailed DFT study on the interactions between a family of quercetin and graphene surface.

## 2. Computational details

Density function theory method is used to calculate the HOMO-LUMO studies using B3LYP method with the basis set 6-21G (d,p) Gaussian 09 software programs [38-40]. The natural bonding orbital calculations were performed by NBO 5.0 program as executed in the Gaussian 09W program at B3LYP method. The total density of states and partial density of states of the QCT-SLG were calculated using multiwfn 3.3 program package [41]. XRD pattern of quercetin with graphene was recorded using an X-ray diffraction instrument (ULTIMA IV, Rigaku diffractometer) employing a cobalt (Co) tube at  $\lambda=1.78\text{\AA}$ , running at 40 kV and 30mA.

## 3. Results and discussion

### 3.1 XRD Measurement

The XRD pattern of quercetin with graphene is shown in Fig.1. The physical mixtures of quercetin with graphene exhibited a number of different peaks; However, these peaks were slightly shifted from their original positions, and also while new peaks were observed. The diffraction pattern for the single layered graphene with quercetin had a broad diffraction peak appearing at 27.02 corresponds to (002) plane, which confirms the short range order in the stacked graphene sheets.

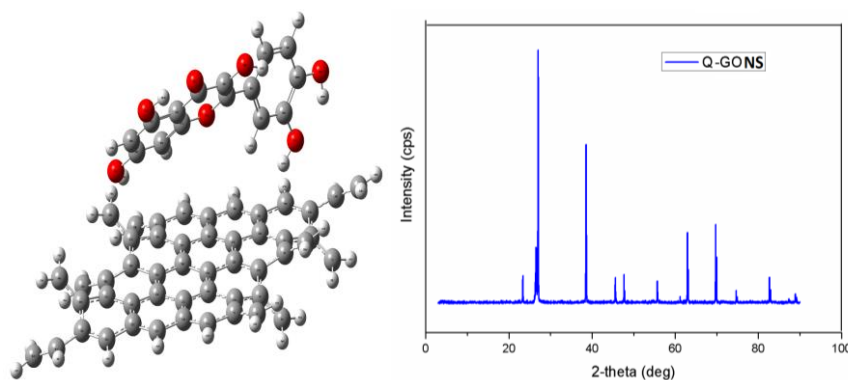


Fig. 1. Molecular structure and XRD pattern of QCT-SLG

### 3.2. Prediction of dipole moment and Hyperpolarizability

The calculated dipole moment and Hyperpolarizability of single layered graphene with quercetin is done by HF method at the basis set of 6-21G(d,p) is shown in table 1. The third rank tensor of the hyperpolarizability can be described by 3D matrix can be reduced to ten components due to Kleinmann symmetry [42]. The energy of the molecular systems is functioned with the presence of external electric field. The  $\beta$  components are described using coefficient in the Taylor series expansion of the energy in the external electric field. The external electric field depends on energy of unperturbed molecules, dipole moment, polarizability and first order hyperpolarizability of the molecules were calculated by finite field of approach and it is expressed as

$$\alpha_{\text{tot}} = \alpha_{xx} + \alpha_{yy} + \alpha_{zz} / 3$$

$$\beta = (\beta_x^2 + \beta_y^2 + \beta_z^2)^{1/2}$$

$$\beta = [(\beta_{xxx} + \beta_{xyy} + \beta_{xzz})^2 + (\beta_{yyy} + \beta_{xxy} + \beta_{yzz})^2 + (\beta_{zzz} + \beta_{xxz} + \beta_{yyz})^2]^{1/2}$$

The dipole moment of the titled of the compound is found to be 3.4060 Debye. The hyperpolarizability of the title of the molecules is  $0.816 \times 10^{-30}$ esu which is five times greater than urea. The NLO effect arises due to interaction of electromagnetic field and titled molecule. The high  $\beta$  value indicates the charge delocalization along the bonding axis and it is clearly show that charge transfer process involves in intermolecular orbital.

Table 1 a) Calculated Dipole moment ( $\mu$ ), polarizability ( $\alpha$ ) and hyperpolarizability ( $\beta$ ) of QCT-SLG by HF/6-31G(d, p) method

$\mu$ value	HF/6-31G(d,p)
$\mu_x$	1.1526
$\mu_y$	-3.1857
$\mu_z$	-0.3516
$\mu$	3.4060

Table 1 b) Calculated polarizability ( $\alpha$ ) and hyperpolarizability ( $\beta$ ) of QCT-SLG by HF/6-31G(d, p) method

$\alpha$ value	HF/6-31G(d, p)	B3LYP	$\beta$ value	HF/6-31G(d,p)
$\alpha_{xx}$	-384.35	-4.1689	$\beta_{xxx}$	112.5887
$\alpha_{yy}$	-398.80	-18.631	$\beta_{yyy}$	94.1437
$\alpha_{zz}$	-357.37	22.8003	$\beta_{zzz}$	8.0490
$\alpha_{xy}$	5.795	5.7955	$\beta_{xyy}$	-2.0360
$\alpha_{xz}$	-2.6897	-2.6897	$\beta_{xxy}$	-139.0528
$\alpha_{yz}$	-1.7999	1.7999	$\beta_{xxz}$	5.2366
Total	-1139.21a.u	4.9061a.u	$\beta_{zzz}$	-0.8072
			$\beta_{yzz}$	15.1263
			$\beta_{yyz}$	-0.9158
			$\beta_{xyz}$	-10.6424
			Total	$0.816 \times 10^{-30}$ esu

### 3.3. HOMO-LUMO analysis

The HOMO-LUMO energies are popular quantum mechanical descriptors which [43] play a major role in governing wide range of chemical interactions. The Frontier Molecular Orbital gives an insight about the reactivity of the molecule and the active site can be demonstrated by the distribution of frontier orbital. The HOMO-LUMO frontier orbital compositions for QCT-SLG calculated with the DFT/6-311G orbital energy level are shown in Fig.2 respectively. In order to evaluate the orbital energy level behavior of the title compounds, the third highest and highest occupied MO's (HOMO and HOMO-3), the lowest and the third values lowest unoccupied MO's (LUMO and LUMO+3) are performed. The electronic absorption spectra corresponds to the transition from molecular orbital were the highest occupied molecular orbital and the lowest unoccupied molecular orbital of title of the compound are alpha molecular orbital level (242) and alpha molecular orbital level (243) respectively. The differences between the orbital energies were shown in table 2. The energy values of HOMO (242) orbital and LUMO (243) orbital were lying at an energy value of -3.7552 eV and 2.5897 eV respectively. The HOMO-LUMO energy gap was obtained at 6.3449 eV in the isolated gas molecular calculations. The HOMO-LUMO energy gap is higher implies the kinetic energy is higher and high chemical reactivity.

Table 2 Theoretical transition levels between HOMO and LUMO and frontier orbital of QCT-SLG were calculated by B3LYP/6-31G (d,p) method

Level	MO Energy (eV)	Level	MO Energy (eV)	$\Delta E$ (eV)
HOMO	-3.7552	LUMO	2.5897	6.3449
HOMO	-3.7552	LUMO+1	3.0939	3.944
HOMO	-3.7552	LUMO+2	4.1769	3.4501
HOMO	-3.7552	LUMO+3	4.737	8.4922
HOMO-1	-4.2667	LUMO	2.5897	2.9282
HOMO-2	-5.2491	LUMO	2.5897	2.8738
HOMO-3	-5.8096	LUMO	2.5897	8.3993
HOMO-1	-4.2667	LUMO+1	3.0939	3.7157
HOMO-2	-5.2491	LUMO+2	4.1769	3.1674
HOMO-3	-5.8096	LUMO+3	4.737	10.5466

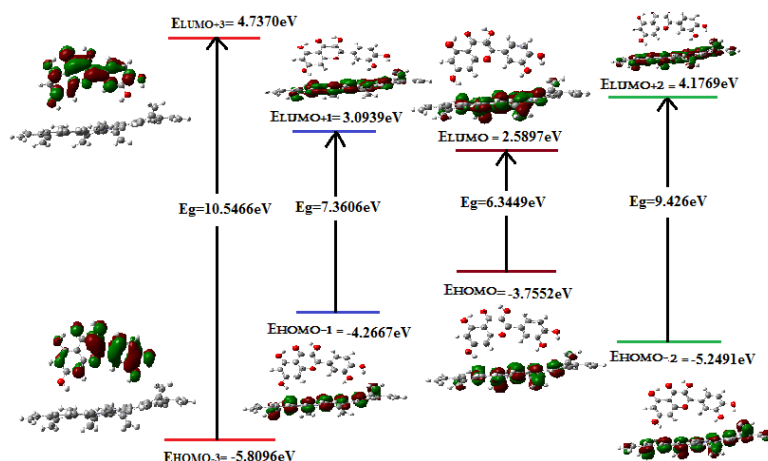


Fig. 2. Frontier molecular diagram of QCT-SLG

### 3.4. Natural Bonding Orbital analysis

The strong intramolecular hyperconjugate interaction takes place between  $\sigma$ C43-C44 and  $\sigma^*$ C31-C32 and hence its electron density value is 1.84 which is present in SLG, whereas the intramolecular hyperconjugate interaction in the ring structure takes place in C88-O79. The natural population analysis of the QCT-SLG shows the Lewis structure 97.73% and non Lewis structure 2.266%. The result shows the charge transfer causing the stabilization occurs within the SLG with respect to QCT.

Table 3. Second Order perturbation theory analysis of Fock matrix in NBO basis for single layered graphene by B3LYP/6-31G (d,p) method

Donor NBO (i)	ED/e	Acceptor NBO (j)	ED/e	E(2) kcal/mol	E(j)-E(i) a.u.	F(i,j) a.u.
C 1 - C 2	1.9215	C 11 - C 12	0.0798	1.33	1.83	0.044
C 7 - C 8	1.9169	C 19 - C 20	0.0819	0.89	1.83	0.036
C 9 - C 10	1.9158	C 19 - C 20	0.0826	0.87	1.84	0.036
C 11 - C 12	1.9164	C 1 - C 2	0.0824	1.05	1.83	0.039
C 11 - C 12	1.9165	C 21 - C 22	0.0823	1.29	1.83	0.043
C 19 - C 20	1.9153	C 9 - C 10	0.0829	1.23	1.85	0.043
C 19 - C 20	1.917	C 29 - C 30	0.0819	1.16	1.83	0.041
C 21 - C 22	1.9223	C 11 - C 12	0.0793	1.23	1.83	0.042
C 21 - C 22	1.9225	C 31 - C 32	0.0799	1.28	1.84	0.043
C 29 - C 30	1.917	C 19 - C 20	0.0818	1.24	1.84	0.043
C 29 - C 30	1.9165	C 39 - C 40	0.0823	1.23	1.83	0.042
C 31 - C 32	1.9165	C 21 - C 22	0.0823	1.15	1.83	0.041
C 31 - C 32	1.9158	C 43 - C 44	0.0826	1.04	1.83	0.039
C 33 - C 34	1.9169	C 21 - C 22	0.0819	1.18	1.83	0.042
C 39 - C 40	1.9215	C 29 - C 30	0.0798	1.29	1.83	0.043
C 43 - C 44	1.8461	C 31 - C 32	0.1563	1	1.84	0.038
C 49 - C 50	1.9864	C 39 - C 40	0.1584	1.34	1.83	0.044
C 8	1.8522	C 8 - C 17	0.1563	0.54	11.71	0.072
C 10	1.9897	C 10 - C 19	0.0799	0.73	11.71	0.083

Donor NBO (i)	ED/e	Acceptor NBO (j)	ED/e	E(2) kcal/mol	E(j)-E(i) a.u.	F(i,j) a.u.
C 19	1.9897	C 19 - C 20	0.1165	0.51	11.96	0.07
C 41	1.9897	C 32 - C 41	0.1193	0.74	11.7	0.084
C 43	1.9897	C 34 - C 43	0.1433	0.5	11.72	0.069
O 79 - C 87	1.9865	C 88 - C 90	0.0099	1.58	1.83	0.048
O 82 - C 91	1.9865	C 86 - C 87	0.01488	1.01	1.9	0.039
O 82 - C 91	1.9865	C 88 - C 90	0.1476	0.89	1.96	0.037
C 87	1.9865	O 79 - C 87	0.1481	1.98	11.71	0.137
C 88	1.9865	O 79 - C 88	0.1193	1.74	11.69	0.128
C 88	1.9897	C 88 - C 90	0.1008	0.6	11.97	0.076
C 89	1.9897	C 88 - C 89	0.0099	0.59	11.7	0.075
C 90	1.9897	O 80 - C 90	0.1165	1.54	11.7	0.12
C 90	1.9897	C 88 - C 90	0.0799	0.53	11.95	0.072
C 92	1.8522	O 81 - C 92	0.1563	1.54	11.75	0.121
C 94	1.8522	O 83 - C 94	0.0068	1.75	11.72	0.129
C 98	1.8373	O 84 - C 98	0.0129	1.84	11.69	0.132
C 100	1.8373	O 85 - C 100	0.0854	1.72	11.71	0.127

### 3.5. MEP Mapping

Molecular electrostatic potential is highly informative concerning the nuclear and electronic charge distribution of the molecules besides it is a tool for interpretation and prediction of chemical reactivity. The MEP has proved to be extremely good for the description of non-covalent interactions particularly hydrogen bonds [44-46]. MEP is widely used as a reactivity map displaying most probable region for nucleophilic and electrophilic attacks. In the MEP surface, red colour refers to electron-rich (negative) region, blue colour refers to electron-poor (positive) region and green colour signifies zero electrostatic potential. In majority of the MEP surfaces, negative region is the preferred site for the electrophilic attack and positive region is preferred for nucleophilic attack. The electron concentrations at the MEP surface are indicated by different colours. The values of electron density increases in the following order

Red > Orange > Yellow > Green > Blue

In QCT-SLG, the electrophilic region occurs in the oxygen which is present in the quercetin molecule. The negative and positive electron density were occurs in the region of  $-2.304 \times 10^{-2}$  a.u. to  $2.304 \times 10^{-2}$  a.u. The MESP at different points on the electron density isosurface is shown by the colour isosurface in the Fig.3. Red colour indicates the strong attraction which occurs in quercetin molecule due to oxygen atoms whereas blue colour which occurs in the overall region of single layered graphene. It is observed that nucleophilic attack is more predominant than electrophilic attack due to C-H molecules in SLG.

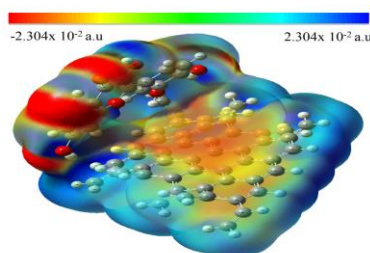


Fig. 3. Molecular electrostatic potential mapping of SLG

### 3.6. Density of states

The important application of DOS plot is to demonstrate the molecular orbital and their contribution of chemical bonding through the OPDOS plot [47]. The DOS plot results show that overlapping population in the molecular orbital. The OPDOS result shows that non bonding, bonding and antibonding interactions between the two orbital atom groups. The positive value of OPDOS indicating that the bonding interaction and negative value indicates the antibonding interactions and zero values indicates the non bonding interactions. The DOS plot gives the composition of group of orbital contributing to the molecular orbital. The PDOS and OPDOS plots are shown in the Fig.4. The plot for DOS is taken from the range of -1.50a.u. to +1.50a.u. The graph exhibits the orbital characteristics of different energy range. It is the major contribution from s orbital and p orbital basic function of carbon in the frontier molecular orbital. The partial density of states (PDOS) of the carbon atom of the title of the molecule exhibits the total density states of the molecules. The OPDOS of the carbon has just larger positive energy then the negative energy values. The carbon atoms which is present in SLG have more energy than the carbon atoms in QCT.

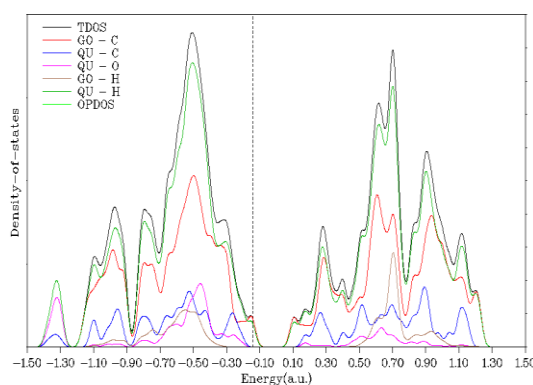


Fig. 4. Total and partial density of states diagram of QCT-SLG

### 3.7. Global chemical reactivity

Density functional theory (DFT) [48] has been found to be successful in providing theoretical insights into the chemical reactivity and selectivity, in terms of qualitative chemical concepts like electronegativity ( $\chi$ ), hardness ( $\eta$ ), softness(S), electrophilicity index( $\omega$ ).The basic relationship of the density functional theory of chemical reactivity is precisely, the one established by Parr et al., [49], that links the chemical potential of DFT with the first derivative of the energy with respect to the n number of electrons, and therefore with the negative of the electronegativity  $\chi$ . Ionization potential (I) is defined as the amount of energy required to remove an electron from a molecule [50]. Electron affinity (A) is defined as the energy released when a proton is added to a system [51]. It is related to the energy of the  $E_{\text{HOMO}}$  and  $E_{\text{LUMO}}$  through the equation:

$$I = -E_{\text{HOMO}} ; \quad A = -E_{\text{LUMO}}$$

When the values of  $I$  and  $A$  are known, one can determine the electronegativity  $\chi$  and the global hardness ( $\eta$ ).The electronegativity is defined as the measure of the power of an atom or group of atoms to attract electrons towards itself [52], Hardness ( $\eta$ ) can be defined within the DFT as the second derivative of the  $E$  with respect to  $N$  as  $\nu(r)$  property which measures both the stability and reactivity. It can be estimated by using the equation:

$$\chi = I + A/2 \quad ; \quad \eta = I - A/2$$

Chemical softness (S) is the measure of the capacity of an atom or group of atoms to receive electrons [53-54], it is estimated by using the equation:

$$S = 1/\eta$$

Parr *et al* [55] have proposed electrophilicity index as a measure of energy lowering due to maximal electron flow between donor and acceptor. They defined electrophilicity index ( $\omega$ ) as follows.

$$\omega = \mu^2/2\eta$$

According to the definition, this index measures the propensity of chemical species to accept electrons. A good, reactive, nucleophile is characterized by lower value of  $\mu$ ,  $\omega$ ; and conversely a good electrophile is characterized by a high value of  $\mu$ ,  $\omega$ . All the global quantities of SLG were calculated.

Table 4 Calculated quantum chemical parameters of SLG-QCT by B3LYP/6-31G(d,p) method

Quantum chemical parameters	B3LYP/6-31G(d,p)
Hardness( $\eta$ )	0.11658eV
Chemical potential( $\mu$ )	-0.11658 eV
Ionization potential(I)	0.1380 kJ/mol
Electron affinity(A)	-0.09517 kJ/mol
Energy gap( $E_g$ )	0.23317 eV
Electrophilicity index	0.5 eV
Chemical softness (S)	8.577

#### 4. Conclusions

The calculated hyperpolarizability of QCT-SLG is a five folders greater compared to the UREA, which shows high chemical reactivity between QCT-SLG. The HOMO-LUMO energy gap of higher order increases which shows the greater chemical reaction between QCT-SLG. The density of states of the QCT-SLG was analyzed and it exhibits the stabilization of the molecules which depends on carbon of SLG. The MESP provides the information on charge density distribution of the QCT-SLG. All the global parameters were calculated and analyzed. The study of theoretical insight can contribute significantly to the understanding of the stability of the QCT with SLG.

#### References

- [1] E. Middelton, C. Kandaswami, in: J.B. Harborne 1994
- [2] T. Leighton, C. Ginther, T. Huang, C.T. Ho, C.Y. Lee (Eds.), ACS, 1992
- [3] P. Hollman, M. Hertog, M. Katan, Food Chem. **57**, 43 (1996).
- [4] B. Havsteen, Biochem. Pharmacol. **32**, 1141 (1983).
- [5] J. K. Wassei, RB Kaner (2013) Acc Chem Res 46:224
- [6] H. Y. Mao, S. Laurent, W. Chen et al. Chem Rev **113**, 3407(2013)
- [7] A. Bianco, Angew Chem Int Ed **52**, 4986 (2013).
- [8] V. Palermo Chem Commun **2013**(49), 2848(2013)
- [9] Y. H. Lu, W. Chen, Y.P. Feng, P.M. He, J Phys Chem B **113**, 2 (2009).
- [10] V. Georgakilas, M. Otyepka, A.B. Bourlinos, V. Chandra, N. Kim, K.C. Kemp, P. Hobza, R. Zboril, K.S. Kim, Chem Rev **112**, 6156 (2012).
- [11] J. Björk, F. Hanke, C.A. Palma, P. Samori, M. Cecchini, M. Persson, J Chem Phys Lett **1**, 3407 (2010).
- [12] S. Gowtham, R.H. Scheicher, R. Ahuja, R. Pandey, S.P. Karna, Phys Rev B **76**, 033401 (2007)
- [13] T.O. Wehling, K.S. Novoselov, S.V. Morozov, E. E. Vdovin, M. I. Katsnelson, A. K. Geim, I. L. Lichtenstein, Nano Lett **8**, 173 (2008).
- [14] S. K. Saha, R. C. Chandrakanth, H. R. Krishnamurthy, Phys Rev B **80**, 15541 (2009).
- [15] L. Tsetseris, S. T. Pantelides, Phys Rev B **85**, 15544 (2012).

- [16] A. J. Samuels, J. D. Carey ACS Nano **7**, 279 (2013).
- [17] J.W. Li, Y.Y. Liu, L.H. Xie, J.Z. Shang, Y. Qian, M.D. Yi, W. Huang, Phys Chem **17**, 491 (2015).
- [18] P.A. Denis, J Phys Chem, **C117**, 389 (2013).
- [19] I.S.S. Oliveira, R.H. Miwa, J Chem Phys **142**, 04430 (2015).
- [20] T. Hu, I.C. Gerber, J Phys Chem C **117**, 241 (2015).
- [21] M.A. Vincent, I.H. Hillier, J Chem Inf Model **54**, 225 (2014).
- [22] D. Mollenhauer, C. Brieger, E. Voloshina, B. Paulus, J PhysChem C **119**, 1898 (2015).
- [23] P.A. Denis, F. Iribarne, J Mol Struct THEOCHEM, **957**, 114 (2010).
- [24] Q. Zhou, L. Yuan, X. Yang, Z. Fu, Y. Tang, C. Wang, H. Zhang, Chem Phys **440**, 80 (2014).
- [25] S.D. Chakarova, E. Schröder, B.I. Lundqvist, D.C. Langreth, Phys Rev Lett **96**, 146107 (2006).
- [26] O. Leenaerts, B. Partoens, R.M. Peeters, Microelectron **40**, 860 (2009).
- [27] I. Hamada, Phys Rev B, **86**, 195436 (2012).
- [28] M. Galicia-Hernández, E. Chigo-Anota, M.T. Romero-de la Cruz, M. González-Melchor, G. Hernández-Cocoletzi, J Mol. Model **18**, 3857 (2012).
- [29] P. Lazar, F. Karlicky, P. Jurecka, M. Kocman, E. Otyepkova, K. Safarova, J Am Chem Soc **135**, 6372 (2013).
- [30] C. Lechner, A.F. Sax, J Phys Chem C **118**, 20970 (2014).
- [31] L. Xu, X. Zhou, W.Q. Tian, T. Gao, Y.F. Zhang, S. Lei, Z.F. Liu, Angew Chem **126**, 1 (2014).
- [32] C. Herrera, R. Alcalde, M. Atilhan, S. Aparicio, Phys Chem C **118**, 9741 (2014).
- [33] Y. Wang, Z. Xu, Y.N. Moe, Chem Phys **406**, 78 (2012).
- [34] Y. Zhao, Z. Hu, J Phys Chem B **117**, 10540 (2013).
- [35] M. Vijayakumar, B. Schwenzer, V. Shutthanandan, J. Hu, J. Liu, I. A. Aksay, Nano Energy **3**, 152 (2014).
- [36] N. Ramos-Berdullas, I. Perez-Juste, C. Van Alsenoy, M. Mandado, Phys Chem Chem Phys **17**, 575 (2015).
- [37] W. Y. Huang, L. Fu, C. Y. Li, L. P. Xu, L. X. Zhang, W. M. Zhang, Journal of Food Science, 1239 (2017).
- [38] B. Miehlich, A. Savin, H. Stoll, H. Preuss, Chem. Phys. Lett. 157 (1987).
- [39] M. Frisch et al, Gaussian an 09 Rev. E. 01, (2009).
- [40] A. Frish, et al, A.B. Gassview, Gaussian Inc., Pittsburgh, PA, 2000.
- [41] Lu Tian, Feiwu Chen, Journal of Computational Chemistry 580 (2012).
- [42] D. A. Kleinman, Physical Review, 1977.
- [43] Z. Zhou, R.G. Parr, J. Am. Chem. Soc., 5720 (1990).
- [44] E. Scrocco, J. Tomasi, Adv. Quantum Chem. 115 (1979).
- [45] F. J. Luque, J.M. Lopez, M. Orozco, Theor. Chem. Acc. 343 (2000).
- [46] N. Okulik, A.H. Jubert, Int. Electron J. Mol. Des. 17 (2005).
- [47] M. Reinboth, S. Wolfram, G. Abraham, F.R. Ungemach, 198 (2010).